

Research Article

Preparation of Starch-Chitosan Nanocomposites for Control Drug Release of Curcumin

Debi Prasan Mohanty[†], S.K Biswal^{†*} and P.L Nayak[‡]

[†]Department of Chemistry, Centurion University of Technology and Management, Odisha, India

[‡]P.L.Nayak Research Foundation, Synergy Institute of Technology, Bhubaneswar, Odisha, India

Accepted 07 Feb 2015, Available online 10 Feb 2015, Vol.5, No.1 (Feb 2015)

Abstract

In the present research program, novel nanocomposites of Starch, which is one of the most abundant polysaccharides polymer, which blended with the Chitosan has been carried out varying the proportion of MMT (Cloisite 30B) were prepared. The blending of the two polymers has been carried out varying the proportion of nanoclay so that the composite can be a better drug carrier. The blends were characterized by Fourier Transmission Infrared Spectroscopy (FTIR), Scanning Electron Microscopy (SEM), Xray Diffraction (XRD) analysis. The swelling studies have been carried out at different drug loading. Swelling study is an important parameter to predict the diffusion of the drugs from the matrix. The kinetics of the drug delivery system has been systematically studied. Drug release kinetics was analyzed by plotting the cumulative release data versus time by fitting to an exponential equation which indicated the non-Fickian type of kinetics. The drug release was investigated at different pH medium, and it was found that the drug release depends upon the pH medium as well as the nature of matrix

Keyword: Starch, Chitosan, Curcumin, Nanocomposite, Drug delivery

1. Introduction

Drug delivery systems (DDS) that can precisely control the release rates or target drugs to a Specific body site have had an enormous impact on the healthcare system. The last two decades in the pharmaceutical industry have witnessed an avant-garde interaction among the fields of polymer and material science, resulting in the development of novel drug delivery systems (Swain, 2005) (Nanda,2007) (Nanda,2007) (Pathak,1992) (Calinescu,2012) (Goyanes, 2011). Carrier technology offers an intelligent approach for drug delivery by coupling the drug to a carrier particle such as microspheres, nanoparticles, liposomes, etc. which modulates the release and absorption characteristics of the drug. Conventional drug administration does not usually provide rate-controlled release or target specificity. In many cases, conventional drug delivery provides sharp increases of drug concentration at potentially toxic levels. Following a relatively short period at the therapeutic level, drug concentration eventually drops off until re-administration (Kundu, 2010) (Ngoenkam,2010) (Calinescu,2008).

A recent survey of the literature reveals that starch/chitosan mixture has been blended with montmorillonite (MMT) has not been used as a carrier

for controlled drug delivery systems. The composite has been blended with different amounts of cloisite 30B to be used for drug delivery. Clay minerals are widely used materials in drug products both as excipients and active agents. (Kim,2009)(Wang,2006)(Musiał,2005) (Heller,2003)(Hoover,2001).

2. Experimental

2.1 Materials

All the reagents used were of analytical purity. Soluble starch was a gift sample from Universal Starch Chem. Allied. Ltd., Mumbai. It was pre-dried in the vacuum oven at 60°C for 10 h. Chitosan (CS) (Degree of Deacetylation = 95% determined by ¹H NMR) was purchased from India Sea Foods, Kerala. MMT (Cloisite 30B) was procured from Southern Clay Products, USA. Curcumin was received as gift sample from Dabar, India. Acetic acid, NaH₂PO₄, NaOH, and other chemicals were used as analytical grade and purchased from Sigma Aldrich Company.

2.2 Synthesis of starch/chitosan /MMT blend

Starch/chitosan /MMT blend films were produced as follows. Starch was dissolved in hot water. Chitosan was dissolved in 0.5M acetic acid. To prepare sterile 1% (w/v) chitosan solutions, chitosan suspension in

*Corresponding author: S.K Biswal

water was first autoclaved (at 121 °C in a wet cycle for 20 min) and then dissolved by adding acetic acid equivalent to 0.5M in a sterile laminar flow hood. The calculated amounts of starch, chitosan, and a little glycerin were mixed at various ratios (Starch content is from 90-60 wt % and chitosan content is from 10-40 wt %), the mixture was slowly added to distilled water at room temperature under continuous stirring. And stirring was maintained for 3 h to completely gelatinize the starch. The volume was maintained by adding water. Calculated amount of MMT (C30B) with three compositions (1%, 2.5%, 5%) were added to 80:20 ratio. When completely suspended the temperature of the mixture was slowly raised to 80°C maintaining stirring. After raising the temperature to 95°C, the mixture was removed from the heat; the foam was skimmed off, and then cast onto level Teflon-coated glass plates. After drying the solution at room temperature, the films were allowed to dry in a hot-air oven at 60°C for 8 h and dried starch/chitosan/MMT films were peeled from the plates. Films were stored in polyethylene bags before use in further studies (Bie, 2013).

2.3 Drug loading

Required amount of Starch/chitosan /MMT (80 : 20) and nanoclay 5% was taken in 5 mL of acetic acid. The mixture was continuously stirred with a mechanical stirrer. Curcumin of different loadings, i.e., 10 wt %, 20 wt %, 30 wt %, 40 wt %, and 50 wt % were then added to the above mixture and stirred for 1 h and then the composites were kept at room temperature for drying (Sarmila, 2009).

2.4 Dissolution experiments

Dissolution experiments were performed at 37°C using the dissolution tester (Disso test, Lab India, Mumbai, India) equipped with six paddles at a paddle speed of 100 rpm. About 900 mL of phosphate buffer solution (pH 3.4 and 7.4) was used as the dissolution media to stimulate gastrointestinal tract (GIT) conditions. A 5 mL aliquot was used each time for analyzing the curcumin content at a fixed time interval (Bie, 2013)(Sarmila, 2009). The dissolution media was replenished with a fresh stock solution. The amount of curcumin released was analyzed using a UV spectrophotometer (Systronics, India) at the λ_{max} value of 524 nm.

3. Characterization

3.1 Fourier Transmission Infrared Spectroscopy (FTIR)

The FTIR spectrum of the Starch/chitosan blends was obtained using a BIORAD-FTS-7PC type FTIR spectrophotometer.

3.2 Thermogravimetric Analysis (TGA)

Thermal degradation pattern of the Starch-Chitosan nanocomposites were studied using TA Instruments TGA- 2950 thermo-gravimetric analyzer. About 5mg of Starch-Chitosan sample was used and scan temperature range was from room temperature to 800°C at 3°C min⁻¹ in air.

3.3 X-Ray Diffraction (XRD)

The change in gallery height of the blend was investigated by WAXD experiments, which were carried out using an X-ray diffractometer (BEDE D-3 system) with Cu K α radiation at a generator voltage of 40 kV and a generator current of 100 mA. Samples were scanned from $2\theta = 1-10^\circ$ at a scanning rate of 2°/min.

3.4 Scanning Electron Microscopy (SEM)

The blending of the Starch/chitosan /MMT composites containing different concentrations were characterized using SEM (440, Leica Cambridge Ltd., Cambridge, UK). The powdered specimens were placed on the Cambridge standard aluminium specimen mounts (pin type) with double-sided adhesive electrically conductive carbon tape (SPI Supplies, West Chester, PA).

3.5 Swelling studies

Water absorption of the polymer-drug conjugates was measured following ASTM D 570-81. The samples were preconditioned at 50°C for 24 h and then cooled in a desiccator before being weighed. The preconditioned samples were submerged in distilled water at 25°C for 24 h. The samples were removed and dried with a paper towel before weighing. Water absorption was calculated as a percentage of initial weight. The soluble material loss was checked by weighting the specimens after drying them in an oven at 50°C for another 24 h. The total water absorption for 24 h was calculated including the soluble material loss.

$$\% \text{ swelling} = \frac{W_1 - W_2}{W_2} \times 100$$

Where, W_1 = weight of swollen composite after 24 h, W_2 = weight of dry composite

4. Results and Discussion

4.1 Fourier Transmission Infrared Spectroscopy (FTIR)

FTIR spectroscopy was used to characterize the interactions between starch and chitosan. The infrared spectra of starch, chitosan, starch/chitosan blend films are shown in (Figure 1.) (Xu, 2005)(Dong, 2004). The starch and chitosan spectra were similar to previous. In the spectrum, the broad band from 3384–3422 cm⁻¹ is due to the OH and/or NH stretching.

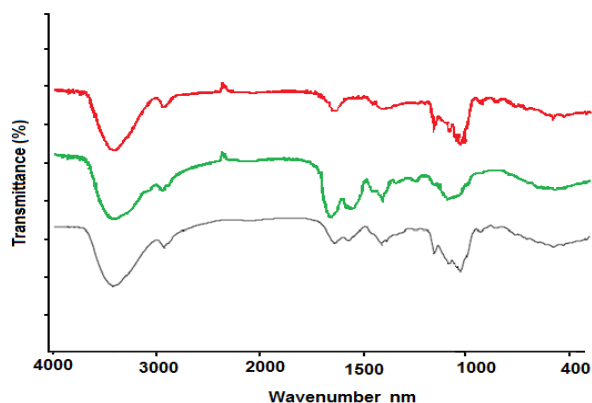


Figure 1 FTIR spectra of Starch, Chitosan (CS), and Starch-Chitosan blend

The band at $2931\text{--}2938\text{ cm}^{-1}$ is due to C–H stretching. The bands from $1630\text{--}1660$ and $1540\text{--}1570\text{ cm}^{-1}$ are the C=O stretching (amide I) and NH bending (amide II), respectively. The peak near 1740 cm^{-1} suggested the presence of a carbonyl group in the starch and chitosan films. The chemical interactions are reflected by changes in the peaks of characteristic spectra after physical blending of two or more substances. This result indicated that interactions were present between the hydroxyl groups of starch and the amino groups of chitosan.

4.2 X-Ray Diffraction (XRD)

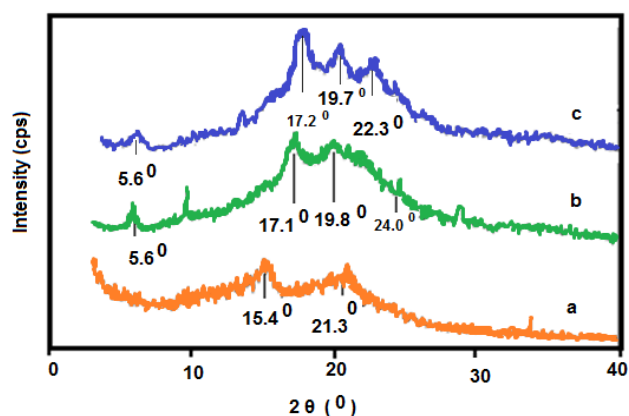


Figure 2 X-ray diffractograms of: (a) free chitosan film, (b) glycerol plasticized Starch film, and (c) starch/chitosan film

The semicrystalline characters of free chitosan film and plasticized starch film are revealed from the diffractograms illustrated in (Figure 2a and b), respectively. The diffractogram of chitosan film presented in (Figure 2a) shows the crystalline peaks (2θ) at 15.3 and 21.18 , which are typical fingerprint for chitosan film. In this study, however, the intensity of the crystal peak at about 21.18 (2θ) is very low, indicating low crystallinity. (Figure 2b) shows the diffraction peak of free starch film at approximately 178 (2θ), which resembles to the characteristic of B-type crystalline structure. From previous study ,

amylase film showed the main peaks at about 5.5 and 178 (2θ) while amylopectin film showed broader reflection around $17\text{--}188$ (2θ). The ordering of B-type structure with water uptake related to the peaks at about 5.5 and 248 (2θ) are the most sensitive to hydration. In addition, the diffraction peak at 19.78 (2θ) is similar to the B-type crystalline peak of amylopectin after storage seven days at 54% RH found in Myllärinen et al.'s work. The observation of the B-type crystalline in the free starch film should be attributed to the fact that crystallization of amylose was developed in the early stage of film formation, whereas that of amylopectin was varied upon the humidity during film formation (Myllärinen, 2002) (Park, 2003).

The X-ray pattern of chitosan-coated starch film displayed in (Figure 2 c) shows reflection of B-type starch crystalline shifting to the slightly higher degrees at about 17.28 (2θ) while that of the chitosan appears as a smaller peak at about 22.28 (2θ). The shifting in starch diffraction peaks may be due to the change in its chain orientation caused by chitosan coating. It is likely that hydrogen bonding interaction between chitosan and starch molecules is responsible for this phenomenon. For chitosan diffraction peak, force and pressure of an automatic film coater probably cause the higher molecular orientation compared to casting technique. In addition, the smaller peak at 5.58 (2θ) and disappearance of peak at 248 (2θ) observed in the diffraction indicate that the amount of water in the coated film was lower than that in the free starch film.

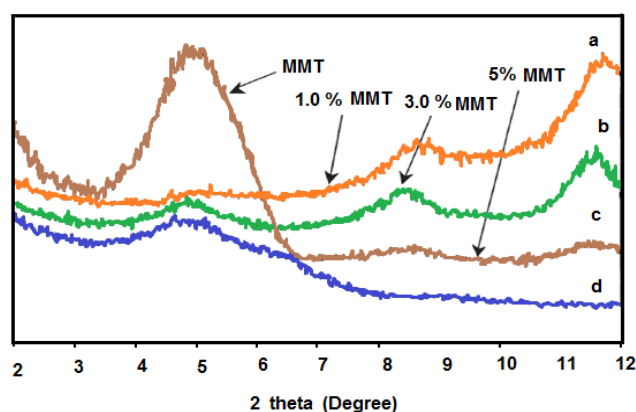


Figure 2 X-ray patterns of MMT and its different amounts of MMT with starch-chitosan blend ; MMT (d); 1% (e); 3% (f); 5% (g)

In (Figure 2 (d, e, f, g)) it shows that when MMT was added to the starch/chitosan solution, irrespective of amount, the peaks remained at the same position ($2\theta = 4.8^\circ$), indicating that no intercalation had occurred, and that microscale composite-tactoids were formed. The formation of different composites with addition of the different clays to chitosan was attributed to the differences in chemical structures and compatibilities with chitosan. MMT had a lower diffraction peak at $2\theta = 4.8^\circ$ ($d_{001} = 18.5\text{ \AA}$) due to replacement of sodium ions with long-chain of quaternary ammonium cations.

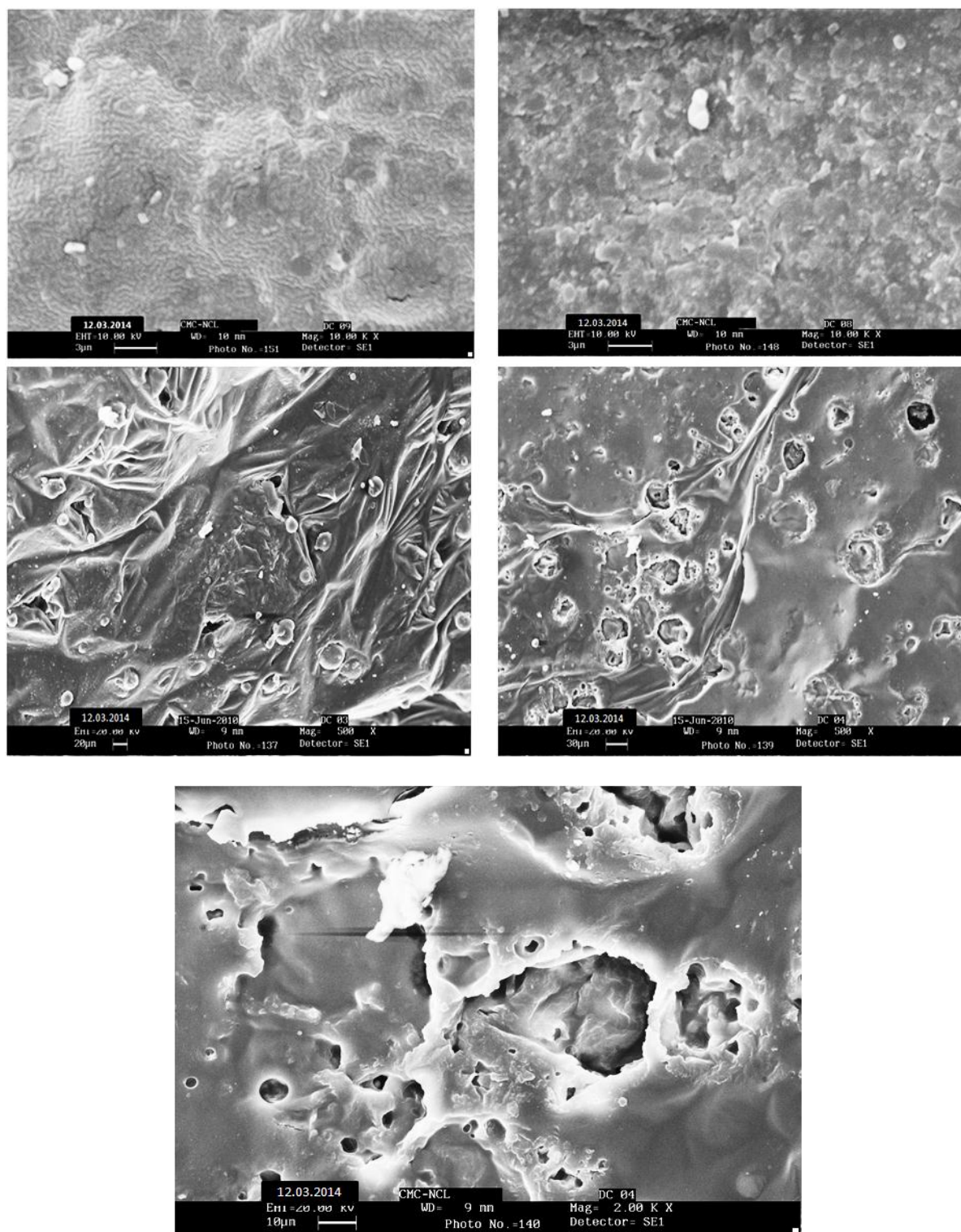


Figure 3 SEM photographs of Starch and Starch/chitosan/MMT nanocomposites. a- Pure starch, b- Starch/chitosan c- Starch/chitosan/1 wt% MMT, d- Starch/chitosan / 2.5 wt% MMT, e- Starch/chitosan /5 wt% MMT

4.3 Scanning Electron Microscopy (SEM)

The scanning electron microscope (SEM) photographs of Starch and Starch/chitosan /MMT nanocomposites were shown in (Figure 3). A comparison of photographs demonstrated that the crystallization behavior of starch was restrained for the existing of

MMT. When the content of MMT was little, the crystallization behavior of starch can hardly be observed. Though the crystallization behavior of starch can still be observed at the high contents of MMT, The dimension of global crystal in starch descend obviously. It reason may be attributed to the small contents of MMT can dispersed well in the matrixes of

starch, while the high contents of MMT tend to agglomerated in starch (Maran,2014).

4.4 Thermogravimetric Analysis

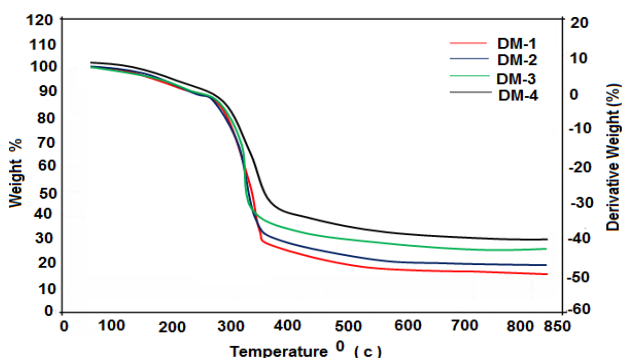


Figure 4 TGA thermogram of Starch-Chitosan Nanocomposites

The thermogravimetric analysis of the sample (DM-01, DM-02, DM-03, DM-04), starch blended with chitosan and MMT has been monitored. The thermal degradation pattern of the samples has been furnished in (Table 1.). The TGA curves of the samples are shown on the (Figure 4). The degradation of the polymer at different temperature is shown on Table 1 A perusal of the degradation pattern of the thermogram indicates that about 4% weight loss observed in case all the polymers at 100°C. This may be due to the moisture absorbed in the samples (Espíndola-González, 2011).

Table 1 Thermal decomposition data of Starch-Chitosan nanocomposites

Sample Code	Percent weight loss at various temperature				
	100°C	200°C	300°C	400°C	500°C
DM-1	5	10	21	75	85
DM-2	4	17	28	71	86
DM-3	3	17	30	67	83
DM-4	4	18	30	65	90

The result indicates that upto 300°C degradation is very slow. The decomposition around 200-300°C is mainly due to a complex process including the dehydration of the polysaccharide rings followed by decomposition of chitosan backbone. The degradation at 400°C is very fast, may be due to breakage of C=C and C-O bonds. The degradation is almost 90% around 500 °C which may be due to elimination CO₂, CO, NH₃, NO₂ etc.

4.5 Moisture absorption

Starch/chitosan with different montmorillonite contents were conditioned at different relative humidity. (Figure 5) shows the changes in the environmental humidity influence the moisture content of Starch/chitosan and Starch/chitosan/MMT.

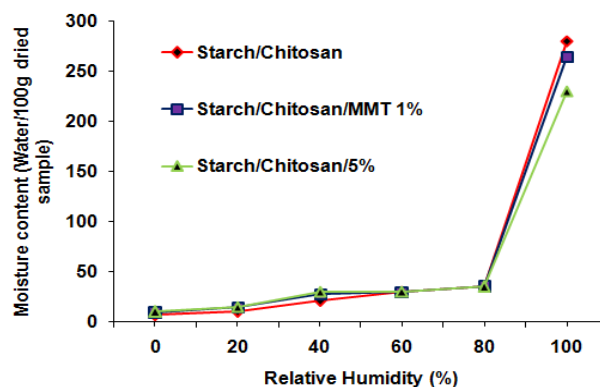


Figure 5 Moisture absorption of starch-clay nanocomposites

The moisture content is unchanged in the nanocomposites compared to the pure polymer for both clay loadings for RH up to 75% (10% and 25% for RH of 43 and 75%, respectively). However, at 96% RH, the nanocomposites show increased moisture content with clay addition. As expected the modulus of starch decreases with increasing RH or moisture content. A similar trend is seen for the nanocomposites. We note that the modulus decrease with increasing RH is not as steep in the nanocomposites. This behavior suggests that the addition of lay to form nanocomposites might prevent property changes during transportation and storage in starch-based products. Starch/chitosan/MMT conditioned at 43% RH show an improvement in modulus compared to the Starch/chitosan. This increase is minimized at 100% RH and 0% RH. While the water uptake is comparable for the neat starch and the nanocomposites, the values diverge at 97% RH. For example the water content for the nanocomposite containing 5% clay is 31% higher than the neat starch. We hypothesize that, at this high water content and because of the hydrophilicity of clay, the water molecules concentrate at the interface resulting in a weaker interface and subsequently lower modulus (Mei, 1999).

4.6 Swelling study

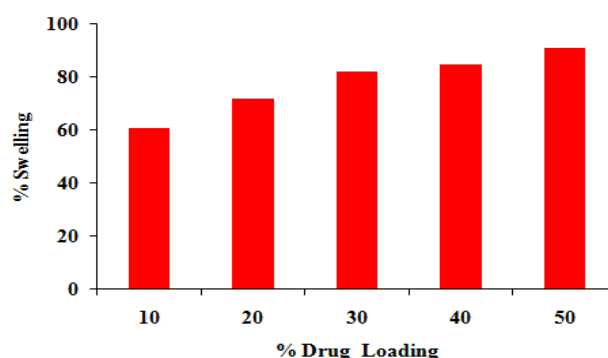


Figure 6 % of Swelling studies of different drug loading of composite starch/chitosan (80:20) +5.0% MMT in 7.4

The swelling behavior of any polymer network depends upon the nature of the polymer, polymer solvent compatibility, and degree of cross-linking. However, in the case of ionic networks, swelling behavior depends upon mass transfer limitations, ion exchange, and ionic interaction. Swelling studies are important to understand the drug release characteristics of the polymer drug conjugate. It depends upon the nature and extent of interaction between solvent molecules and polymer chains in addition to porosity of the polymer and the nature of hydrophilic groups present on the polymer. Here the percentage of swelling increases with increase in the percentage of drug loading in Starch/chitosan /MMT nanocomposites (Yang, 1999).

4.6 In vitro drug release

The drug delivery system was developed for the purpose of bringing, up taking, retaining, releasing, activating, localizing, and targeting the drugs at the right time period, dose, and place. (Frank, 1993) (Langer, 1990). The biodegradable polymer can contribute largely to this technology by adding its own characters to the drugs.

Effect of pH

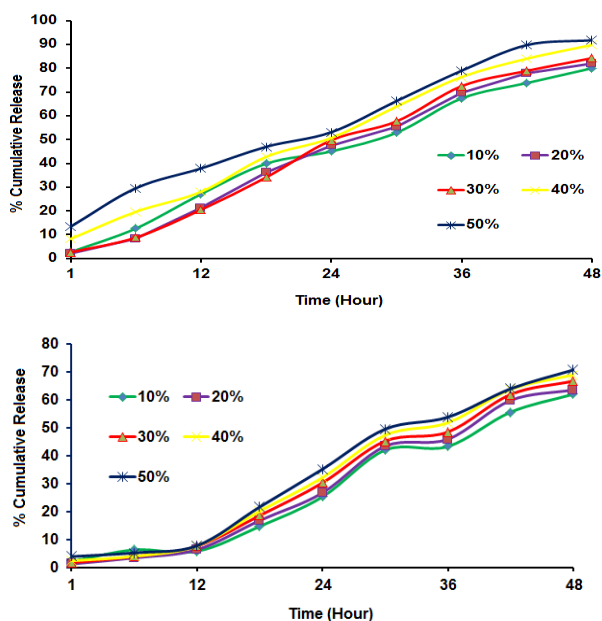


Figure 7 Percentage of cumulative release versus time for different formulation loaded with starch/chitosan (80:20) +5.0% MMT nanocomposites in pH 7.4 and pH 3.4 media.

To investigate the effect of pH on the swelling of composite Starch/chitosan /MMT 1%, we have measured the percentage of cumulative release in both pH 3.4 and 7.4 media. Cumulative release data presented in Figure 7 a,b indicate that by increasing the pH from 3.4 to 7.4, a considerable increase in the cumulative release is observed for all composites.

From Figure 7(a,b), it is seen that the 50% drugpolymer composites have shown longer drug release rates than the other composites. Thus, drug release depends upon the nature of the polymer matrix as well as pH of the media. This suggests that the drugs in the blend can be used to be suitable for the basic environment of the large intestine, colon, and rectal mucosa for which there are different emptying times (Lewis, 1990).

4.7 Effect of time

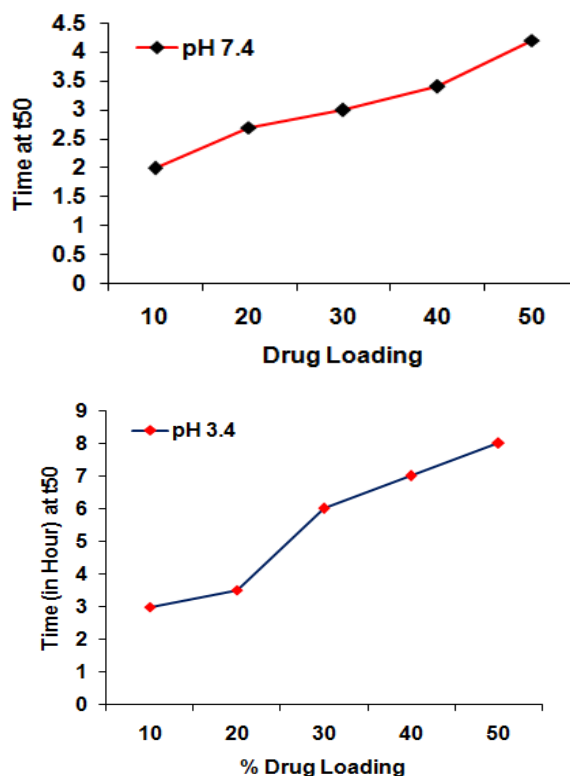


Figure 8 Drug release at time t50 versus drug loading in Starch/chitosan /MMT nanocomposites at (A) pH 7.4 and (B) pH 3.4

Interestingly, curcumin is being released more rapidly at pH 7.4 than at pH 3.4, the release half times t50 (time required for releasing 50 wt % of drug) for 10, 20, 30, 40, 50% drug loading are 2.05, 2.08, 3.0, 3.01, and 4.0 h at pH 7.4, and 3.0, 3.05, 6.0, 7.0, and 8.0 h at pH 3.4, respectively are shown in Figure 8(a,b). More than 80 wt % curcumin is released from composites at pH 7.4 within 8 h, whereas less than 44 wt % of the drug is released at pH 3.4 within 4 h. This suggests that the drugs in the composites can be used to be suitable for the basic environment, further the electrostatic interaction of composites is more easily broken at pH 7.4 than at pH 3.4, leading to curcumin being released more rapidly at pH 7.4 than 3.4. (Heller, 1987).

Effect of drug loading

Figure 9 displays the release profiles of drug from composites at different amounts of drug loadings.

Release data show that formulations containing highest amount of drug (50 %) displayed fast and higher release rates than those formulations containing a small amount of drug loading. The release rate becomes quite slower at the lower amount of drug in the matrix, due to the availability of more free void spaces through which a lesser number of drug molecules could transport (Xu,1995)(Ritger,1987).

4.8 Drug release kinetics

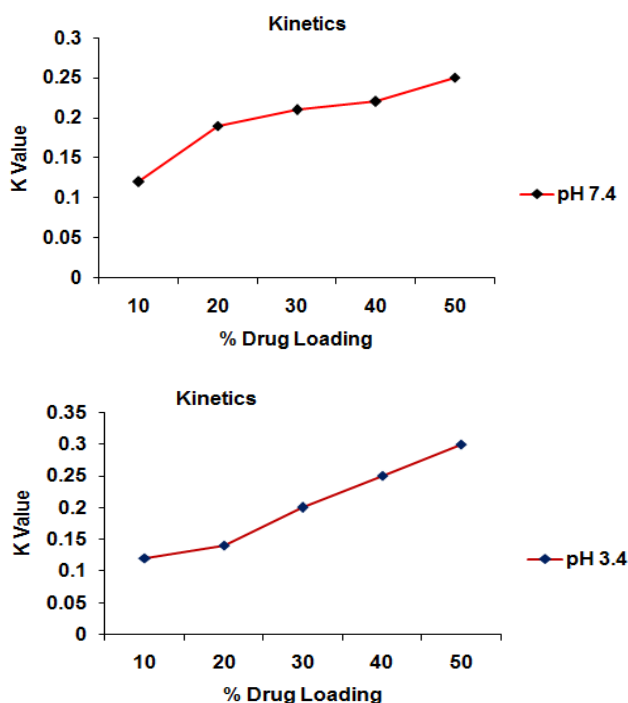


Figure 9 Values of K versus percentage of drug loading in Starch/chitosan/MMT nanocomposites at pH 7.4 (A) and pH 3.4 (B).

4.9 Drug release mechanism from matrices

From time to time, various authors have proposed several types of drug release mechanisms from matrices. It has been proposed that drug release from matrices usually implies water penetration in the matrix, hydration, swelling, diffusion of the dissolved drug (polymer hydro fusion), and/or the erosion of the gelatinous layer. Several kinetics models relating to the drug release from matrices, selected from the most important mathematical models, are described over here. However, it is worth mention that the release mechanism of a drug would depend on the dosage from selected, pH, nature of the drug, and, of course, the polymer used.

Power law equation (diffusion/ relaxation model)

$$M_t/M_\infty = k_5 t^n$$

M_t/M_∞ is the fractional drug release into dissolution medium and k_5 is a constant incorporating the

structural and geometric characteristics of the drug. The term 'n' is the diffusional constant that characterizes the drug release transport mechanism. When $n = 0.5$, the drug diffuses through and is release from the polymeric matrix with a quasi-Fickian diffusion mechanism. For $n > 0.5$, an anomalous, non-Fickian drug diffusion occurs. When $n = 1$, a non-Fickian, Case II or zero-order release kinetics could be observed. Drug release kinetics was analyzed by fitting to an exponential equation of the type as represented below. Here, M_t/M_1 represents the fractional drug release at time t, k is a constant characteristic of the drug-polymer system, and n is an empirical parameter characterizing the release mechanism. Using the least squares procedure, we have estimated the values of n and k for all the five formulations and these data are given in Table 2. The values of k and n have shown a dependence on the, percentage of drug loading and polymer content of the matrix. Values of n for composites prepared by varying the amounts of drug containing 10, 20, and 30 wt % and suggesting shift of drug transport from Fickian to anomalous type. However, the drug-loaded composites exhibited n values ranging from 0.96–1.57 (Table 2), indicating a shift from erosion type release to a swelling controlled, non-Fickian type mechanism. The value of n more than 1 has also been recently reported.^{49,50} This may be due to a reduction in the regions of low micro viscosity inside the matrix and closure of microcavities during the swollen state of the polymer. Similar findings have been found elsewhere, wherein the effect of different polymer ratios on dissolution kinetics was investigated.(Higuchi,1963) (Kulkarni, 1999).

Table 2: Release Kinetics parameter of Different Formulation at pH 7.4 and pH 3.4

Sample Code (wt %)	k		n		Co-orientation Coefficient, R	
	pH 7.4	pH 3.4	pH 7.4	pH 3.4	pH 7.4	pH 3.4
10	0.13	0.10	1.12	1.34	0.9724	0.9307
20	0.18	0.12	1.24	0.82	0.9686	0.9915
30	0.22	0.19	0.96	1.4	0.9881	0.9655
40	0.23	0.24	1.7	1.32	0.9656	0.9305
50	0.24	0.30	1.03	0.73	0.9724	0.9911

Conclusion

In the biodegradation study, both starch/ chitosan and Starch/ chitosan /MMT, the weight loss, which indicated the extent of biodegradation of the blends, increased as the content of chitosan increased. The greater biodegradation of Starch/ chitosan may be caused by the same factors that lead to its higher absorption of water. The percentage of swelling increases with increase in the percentage of drug loading. The drug release depends upon the nature of the polymer matrix as well as pH of the media. The kinetics of the drug release has been investigated. The

values of k and n have been computed. Based on the values of n non-Fickian kinetics has been predicted.

References

- Bie P, Liu P, Yu L, Li X, Chen L, Xie F. (2013) The properties of antimicrobial films derived from poly(lactic acid)/starch/chitosan blended matrix. *Carbohydr Polym.* 98(1):959-66.
- Calinescu C, Mateescu MA (2008) Carboxymethyl high amylose starch: Chitosan self-stabilized matrix for probiotic colon delivery. *Eur J Pharm Biopharm.* 70(2):582-9.
- Calinescu C, Mondovi B, Federico R, Ispas-Szabo P, Mateescu MA. (2012) Carboxymethyl starch: Chitosan monolithic matrices containing diamine oxidase and catalase for intestinal delivery. *Int J Pharm.* 428(1-2):48-56.
- Dong, Z.F., Du, Y.M., Fan, L.H., Wen, Y., Liu, H., and Wang, X.H., (2004) Preparation and properties of chitosan/gelatin/nano-TiO₂ ternary composite films, *J. Funct. Polym.*, **17**, 61-66
- Espíndola-González A, Martínez-Hernández AL, Fernández-Escobar F, Castaño VM, Brostow W, Datashvili T, Velasco-Santos C (2011) Natural-Synthetic Hybrid Polymers Developed via Electrospinning: The Effect of PET in Chitosan/Starch System. *Int J Mol Sci.* 12(3):1908-20.
- Frank, S.; Lauterbur, P. C. (1993) *Nature*, 363, 334.
- Goyanes A, Souto C, Martínez-Pacheco R. A (2011) comparison of chitosan-silica and sodium starch glycolate as disintegrants for spheronized extruded microcrystalline cellulose pellets. *Drug Dev Ind Pharm.* 37(7):825-31.
- Heller, J. Domb and Abraham, J., (2003) "Recent developments with biodegradable polymer", *Adv. Drug Dev. Review.*, **55**, 445-446.
- Heller, J.; Robinson, J.; Lee, J. R. (1987) *Controlled Drug Delivery Fundamentals and Applications*; Marcel Dekker: New York, 139-212.
- Higuchi, T. (1963) *J Pharm Sci*, 52, 1145.
- Hoover, R., (2001) "Composition, molecular structure, and physicochemical properties of tuber and root starches: a review", *Carbohydrate Polymers.*, **45**, 253-267.
- Kim DH, Kim KN, Kim KM, Lee YK. (2009) Targeting to carcinoma cells with chitosan- and starch-coated magnetic nanoparticles for magnetic hyperthermia. *J Biomed Mater Res A.* ;88(1):1-11.
- Kulkarni, A. R.; Soppimath, K. S.; Aminabhavi, T. M. (1999) *Pharm Acta*, 74, 29.
- Kundu B, Lemos A, Soundrapandian C, Sen PS, Datta S, Ferreira JM, Basu D. (2010) Development of porous HAp and β -TCP scaffolds by starch consolidation with foaming method and drug-chitosan bilayered scaffold based drug delivery system., *J Mater Sci Mater Med.* (11):2955-69
- Langer (1990) *R. Science*, 249, 1527.
- Lewis, D. H.; Chasin, M.; Langer, R. Marcel Dekker (1990): New York; Vol. 45, pp 1-8. AQ14
- Lyu, S. P.; Sparer, R.; Hobot, C.; Dang, K. (2005) *J Controlled Release* 102, 679.
- Maran JP, Sivakumar V, Thirugnanasambandham K, Sridhar R (2014) Degradation behavior of biocomposites based on cassava starch buried under indoor soil conditions. *Carbohydr Polym.* ,101:20-8. Mei J, Yuan Y, Guo Q, Wu Y, Li Y, Yu H. (2013) Characterization and antimicrobial properties of water chestnut starch-chitosan edible films. *Int J Biol Macromol.* 61:169-74
- Musił W, Kubis A. (2005) Biodegradable polymers for colon-specific drug delivery. *Polim Med.*;35(4):51-61.
- Myllarinen, P.; Buleon, A.; Lahtinen, R.; Forssell, P. (2002) The crystallinity of amylose and amylopectin films. *Carbohydr. Polym.*, 48, 41-48.
- Nanda, P. K.; Rao, K. K.; Nayak, P. L. (2007) *J Appl Polym Sci*, 103, 31.
- Nanda, P. K.; Rao, K. K.; Nayak, P. L. (2007) *Polym Plast Technol Eng*, 46, 207.
- Ngoenkam J, Faikrua A, Yasothornsrikul S, Viyoch J. (2010) Potential of an injectable chitosan/starch/beta-glycerol phosphate hydrogel for sustaining normal chondrocyte function. *Int J Pharm.* , 391(1-2):115-24.
- Park, H., Lee, W., Park, C., Cho, W., and Ha, C., (2003) Environmentally friendly polymer hybrids part 1 Mechanical, thermal and barrier properties of thermoplastic starch/clay nanocomposites", *Journal of Materials Science.*, 38, 909-915.
- Pathak, C. P.; Sawhney, A. S.; Hubbell, J. A. (1987) *J Am Chem Soc* 1992, 114, 8311.
- Sarmila Sahoo, Debasish Sahoo, Abhisek Sasmal, Padmalochan Nayak (2009) Synthesis and Characterization of Chitosan- Polycaprolactone Blended with Organoclay for Control Release of Doxycycline *Journal of Applied Polymer Science*, 45,23-45
- Swain, S. N.; Rao, K. K.; Nayak, P. L. (2005) *Polym Int*, 54, 739.
- Wang Q, Zhang N, Hu X, Yang J, Du Y. (2007) Chitosan/starch fibers and their properties for drug controlled release. *Eur J Pharm Biopharm.* 66(3):398-404.
- Xu, G. J.; Sunada, H. (1995) *Chem Pharm Pharm Bull*, 43, 483.
- Xu, Y.X., Kim, K.M., Hanna, M.A., and Nag, D., (2005) Chitosan-starch composite film: Preparation and characterization", *Ind. Crops Prod.*, 21, 185-192.
- Yang, G. L.; Feng Zhaang, G. L. (1999) *J Membr Sci*, 161, 31.